Preliminary study of the Hg retention on Au/C regenerable sorbents

M.T. Izquierdo[1*], D. Ballestero[2], R. Juan[1], E. Segura[1], C. Ruiz[1], B. Rubio[1], R. Pino[2]
[1]Instituto de Carboquímica, CSIC. c/Miguel Luesma, 4. 50018 Zaragoza. Spain.
[2]Universidad San Jorge. Autovía A23 Zaragoza-Huesca km 510. 50830 Villanueva de Gállego, Zaragoza. Spain.
mizq@icb.csic.es

Abstract

Mercury (in elemental and oxidized forms) is released during the combustion of fossil fuels. Electrical power plants are estimated to account for about 25% of the global anthropogenic mercury emissions to the atmosphere. Current technologies used to control Hg emissions are able to retain elemental and oxidized Hg but large amount of toxic wastes are obtained during these abatement processes.

In this work, a regenerable sorbent for Hg retention based on carbon supported Au nanoparticles has been developed. In order to avoid pressure drop and particle entrainment honeycomb structures were chosen. Carbon-based supports were chosen because the possibility to modify the surface chemistry to favour the Au dispersion. On the other hand, the capability of Au for Hg retention is based on the amalgamating and deamalgamating property of Hg for Au. Preliminary results of Hg retention and regeneration are obtained in a bench scale experimental installation working at high space velocities 53000 h^{-1}, 120ºC for retention temperature and at Hg inlet concentration of 22 ppbv.

1. Introduction

The largest source of mercury to the atmosphere in the world is the burning of fossil fuels, primarily coal. Electrical power plants are estimated to account for about 25% of the global anthropogenic mercury emissions to the atmosphere and industrial and residential heating for another 20% [1].

In 2005 the USA Environmental Protection Agency (EPA) established “The Clean Air Mercury Rule” turning the United States into the first country to regulate these emissions [2]. On the other hand, the European Commission published in 2005 the “Community Strategy Concerning Mercury”, which identifies coal combustion as one of the main sources of anthropogenic mercury also in Europe [3]. According to the European Environmental Agency (EEA), Spain is the third country among EU27 in mercury emissions, mainly due to coal-fired plants [4].

Mercury is found in coal in the form of sulphides or associated to them, interchanged on clays and associated to the organic matter in low rank coals. During the combustion processes, these forms evaporate, giving rise to Hg (0), HgO and $HgCl_2$, which proportions in gas phase depend on the concentration and mode of occurrence in the coal and on the

compounds present in the gaseous stream, especially particulates and HCl [5]. In some cases, more than 90% of the Hg in coal can be emitted in gas phase through the stack.

The state of the art technology that has shown promise for controlling element as well as oxidized mercury is active carbon injection (ACI). Generally, ACI technologies require a high C:Hg ratio to achieve the desired mercury removal level (> 90%), which results in a high portion cost for sorbent material. The high C:Hg ratio means that ACI does not utilize the mercury sorption capacity of carbon powder efficiently. A major problem associated with ACI technology is its cost. If only one particle collection system is used, the commercial value of fly ash is sacrificed due to its mixing with contaminated activated carbon powder. So, a system with two separate powder collectors and ACI between the first collector for fly ash and the second collector for activated carbon powder would be necessary. The forthcoming regulation of Hg emissions in the UE and the limited residue production due to be accomplished by any depuration technology, make the development of new processes mandatory.

Regenerable sorbents can accomplish high mercury retention that can be recovered as well as balance cost because of its regenerability. Recognizing reversible characteristics of mercury amalgamate with gold and silver, gold- or silver-coated silica beads have been widely used to pre-concentrate low concentration of elemental mercury for its detection [6, 7]. The gold- or silver-mercury amalgam is extremely stable at room temperature. However, the amalgam decomposes to release mercury to a gas phase at higher temperatures, leaving clean gold or silver surfaces ready for further mercury capture [7]. To effectively collect trace amounts of mercury, it is necessary to have the gold and/or silver in a form of large surface areas [8]. The gold and silver in monolayer is effective in mercury capture [9]. The challenge with this design is that with repetitive exposure to flue gases and heating, the coated gold or silver layer tends to aggregate into larger islands in micrometer sizes, which could lead to inefficient mercury capture [7, 8, 10]. Some tests of capture and regeneration are found in the literature [7, 11]. However, both studies performed mercury adsorption at room temperatures much lower than coal-fired power plant flue gas temperatures.

In this work, a preliminary study of Hg retention and regeneration on Au-based sorbents has been carried out. On one hand, in order to avoid pressure drop and particle entrainment structured carbon monoliths were used as support for Au. On the other hand, in order to enhance the efficiency of the sorbents for mercury retention, nanometric Au was deposited on the supports following two different methodologies.

2. Experimental

2.1. Regenerable sorbents

Honeycomb structured carbon monoliths were used as supports. Raw support (labelled MC-orig) has square channel with a density 69 cell/cm^2. Different treatments were applied to the raw support in order to modify the surface chemistry to improve further dispersion of gold nanoparticles. Raw supports were oxidized with either nitric acid (labelled MC-HNO3) or air (labelled MC-air). Raw supports were also steam activated (labelled MC-vapor). These procedures are described elsewhere [12].

Two different methods for gold deposition onto the supports have been used. In colloidal gold method (based in [13]), citrate anion acts as reducing agent of the gold salt and a protector of the gold sol formed preventing its aggregation. The second method consists of the direct reduction of a gold salt by the own carbon material of the support (patent pending). In both methods it is necessary to force the gold suspension/solution to pass through the channels of the monolithic support to try to achieve a homogeneous deposition of gold along the channels of the monolithic supports.

After gold deposition, a reducing treatment was applied to the sorbents. A gas mixture containing 4%H_2/Ar was passed through the sorbent at 300ºC during 1h. Samples coming from gold salt deposition were labelled adding to the support label -Au–SHC (for sorbent with high Au content on the surface) and -Au–SMC (for sorbent with medium Au content on the surface). Samples coming from the colloidal method were labelled adding to the support label -Au–C2.

2.2. Characterization of sorbents

Before gold deposition, supports were characterized by elemental analysis, infrared spectroscopy (FTIR), N_2 physisorption and thermal programmed desorption (TPD). After gold deposition, sorbents were characterized by scanning electron microscopy (SEM), Field Emission SEM (FE-SEM) and N_2 physisorption.

Infrared spectra were obtained on KBr discs (120 mg, 1% weight of monolith) co-adding 512 scans at 4 cm^{-1} resolution. That high number of scans was necessary due to the low infrared response of carbon materials. In order to know the oxidation degree along of CM channels the monoliths were cut lengthwise and FTIR spectra of 0.6x0.4 mm areas on channels were obtained by reflection using a microscope coupled to FTIR spectrophotometer.

Surface areas were determined with N_2 at 77K. The Brunauer-Emmett- Teller (BET) equation was applied to N_2 adsorption isotherms. Prior each analysis samples were outgassed at 150ºC and up to a vacuum less than 10^{-5} mm Hg.

The TPD runs were carried out with a custom built set-up, consisting of a tubular quartz reactor placed inside an electrical furnace. TPD experiments were carried out by heating the samples up to 1100ºC in Ar flow at a heating rate of 10ºC /min, recording the amounts of CO and CO_2 evolved at each temperature with a quadrupole mass spectrometer from Pfeiffer. The calibrations for CO and CO_2 were carried out by standards diluted in Ar. In a typical run 0.5 g of carbon was placed in a horizontal quartz tube reactor under a stream of 30 ml/min of Ar.

The study of the distribution of gold along the monolith channels was carried out by SEM and the particle size distribution was determined by image analysis from electron micrographs obtained from FE-SEM.

2.3. Mercury retention experiments

A bench scale installation (Figure 1) was used to determine the efficiency of the sorbent for the capture of mercury and the maximum retention capacity. This installation consists of two flowmeters for nitrogen, a permeation tube for mercury (inside a tube immersed in a thermostatic bath), a quartz reactor heated by a furnace and an on-line elemental mercury analyzer (VM3000). Moreover, the installation is provided with a tail-end train of flasks to allow the capture the mercury as well as its speciation (in the case of evidences of oxidation

under the experimental conditions). The installation is built up with Teflon pipes and pieces (in the part of the installation where Hg is present) to prevent possible mercury attack to steel.

The Hg breakthrough curves were obtained at space velocity 53000 h^{-1}, 120ºC and Hg inlet concentration of 22 ppb. The total amount of Hg retained was calculated from the integration of the curve. Some experiments were repeated to test reproducibility.

In order to test best regeneration temperature, Hg temperature programmed desorption (Hg-TPD) of exhausted sorbents was performed on some selected samples. Mercury exhausted sorbent was heated up to 450ºC with a heating rate of 10ºC/min, and the Hg evolution was followed on line as a function of the temperature.

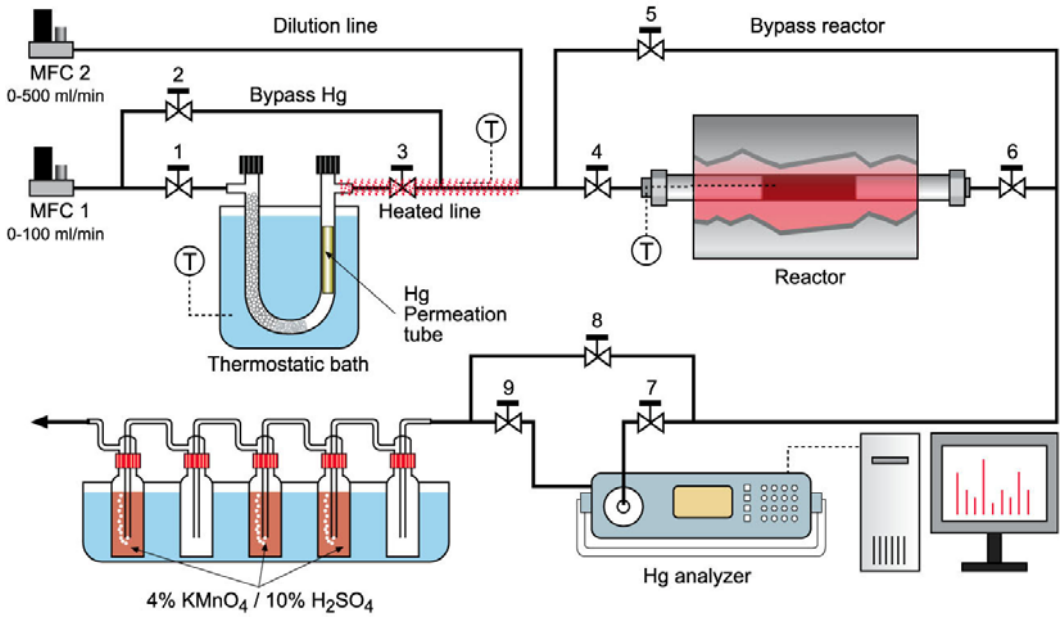

Figure 1. Experimental installation for Hg retention tests.

3. Results and Discussion

3.1. Characterization of the supports

Table 1 summarizes the results from characterization of the supports. As it can be observed from elemental analysis, the level for introduction of oxygen in the structure of the raw support (MC-orig) is similar for acid-oxidation and steam activation treatments and lower for air-oxidation.

Steam activation develops the porous structure of the monoliths and surface area and pore volume are higher than that measured for raw support. Pore volume corresponding to mesopores was calculated with Barret-Joyner-Halenda equation applied to the desorption branch of the N_2 isotherm. Total pore volume was taken at pressures p/p_0=0.995. As can be deduced from Table 1, supports are mainly microporous. Air oxidation of raw support does not alter significantly porous structure and surface area. However, acid oxidation alters the porosity of the support, decreasing the surface area as well as the total pore volume. It is generally reported that the liquid phase oxidation does not change significantly the texture of the activated carbons [14], although under more drastic conditions (concentrated acid, heating

until complete evaporation) a decrease in the surface and pore volume has been observed [14] due to the collapse of pore walls. Steam activation develops the existing porosity, increasing BET surface area as well as mesopores and total pore volume.

Table 1. Characteristics of the supports

	MC-orig	MC-HNO3	MC-air	MC-vapor
Elemental analysis				
C (%)	93.86	68.40	88.16	74.66
H (%)	0.80	1.53	0.82	1.49
N (%)	0.25	1.36	0.00	0.19
S (%)	0.00	0.00	0.00	0.00
O (%, by diff)	5.09	28.71	11.02	23.66
N_2 physisorption				
S_{BET} (m^2/g)	430	343	433	750
V_{meso} (cm^3/g)	0.008	0.006	0.011	0.035
V_p (cm^3/g)	0.251	0.204	0.253	0.448
IR integrated area (region)				
1700 cm^{-1}	0.02	0.92	0.43	0.96
1100 cm^{-1}	4.1	11.27	10.46	6.66
TPD experiments				
CO_2 (mmol/g)	0.313	3.923	0.583	1.054
CO (mmol/g)	1.187	2.821	2.628	2.212

FTIR spectra recorded along channels by reflection technique with infrared microscope suggested that a homogeneous oxidation had occurred along the channel surfaces. Once this fact was tested, spectra of the different supports were collected. Particular attention was focused on the bands at 1700 cm^{-1} due to C=O stretching vibration in carboxylic acids, quinones and lactones, and 1100cm^{-1} associated to C-O stretching vibration in alcohol/phenol groups and/or ether type structures. The absorbance of both bands were integrated, taken into account the sample factor in the pellet (sample/BrK), and the results are given in Table 1.

FTIR study shows a higher formation of surface oxygen groups for nitric oxidation and air oxidation and lower for steam activated support, while elemental analysis shows similar incorporation of oxygen for nitric oxidation and air oxidation. Because of FTIR is a surface technique and elemental analysis and TPD are bulk techniques, the comparison of data corresponding to theses techniques does not infer a contradiction. In the case of steam activated support, the increase of the porosity can lead to the distribution of oxygen surface groups on internal porous, do not visible by FTIR. On the other hand, it should be noted that intensity of IR absorption bands is affected not only by the content of the corresponding functional groups but also for the freedom rate of vibration for the atoms in those groups (this last is especially important for condensed structures such as carbon materials).

The conditions used to oxidize the raw support change the amount and type of surface oxygen functional groups present on the resulting supports. The amounts of CO and CO_2 desorbed and the temperatures at which these gases released have been found to be characteristics of various oxygen functional groups. It has been proposed that CO_2 derives from functional groups like carboxylic acids, anhydrides and lactones and CO derives from functional groups like phenolic and quinonic groups. Groups yielding CO_2 have been shown to decompose typically over a range of temperatures 150º-600ºC while groups yielding CO decompose at temperatures in the range of 600º-1000ºC [15].

The total amount of CO and CO_2 evolved up to 1100ºC in a TPD run for each activated carbon is reported in Table 1. As can be deduced, three treatments (nitric acid, air or steam) increase the amount of total oxygen groups present in the supports. The introduction of CO-evolving groups is similar for the three supports; however the introduction of CO_2-evolving groups is much higher for support MC-HNO3. This fact is important to consider, because it is reported that the deposition of some metals on carbon supports, in particular gold, seems to be favoured by carboxylic-type surface groups [16].

3.2. Characterization of the sorbents

Surface area of the sorbents does not vary significantly after gold deposition, as can be seen comparing supports and sorbents surface area values in Tables 1 and 2. This fact is indicative of non-pore blockage due to Au nanoparticles deposition.

The study of the distribution of gold along the monolith channels was carried out by SEM-EDX. The Au content along the channels was determined and some heterogeneity in Au content along the channels was found. Table 2 shows the Au content for each sorbent as average.

FE-SEM microphotographs (Figure 2) were used to obtain the fraction of surface covered by gold, the Au particle Feret diameter distribution and the circularity of the particles using Image Analysis software. Average for these parameters is reported in Table 2. For sorbent MC-orig-Au-SHC only the fraction of surface covered by gold can be obtained; as can be seen in Figure 2, Au particles are agglomerated, creating big and connected clusters, making impossible to calculate the particle diameter.

Table 2. Surface area, surface Au content (by SEM-EDX) and results from image analysis of FE-SEM micrographs

Sorbent	S_{BET} (m^2/g)	Au (SEM-EDX) (%)	Au surface coverage (%)	Au average particle size (nm)	Au particle average circularity
MC-orig-Au-C2	427	0.83±0.20	4.5	21	0.90
MC-HNO3-Au-C2	n.d.	1.82±0.49	19.4	25	0.86
MC-air-Au-C2	n.d.	0.81±0.22	3.7	19	0.90
MC-vapor-Au-C2	n.d.	1.62±0.47	8.6	20	0.88
MC-orig-SHC	413	8.92±1.18	63.5	-	-
MC-orig-SMC	421	1.94±0.64	26.7	33	0.84

n.d. not determined

There is a straightforward correlation between Au surface coverage and the Au particle diameter, indicating the tendency of Au particles to be sintered when particles are close up enough. The amount of Au loaded on the support surface has a big influence on the Au particle diameter. When the surface fraction covered by Au is too high, the size of particle increases and this fact favours the sintering of the Au particles, reaching the formation of big clusters in the case of sorbent MC-orig-Au-SHC. However, there is not a direct correlation between the Au content and the particle size or surface coverage, but the trend is the higher Au content, the higher Au particle size and surface coverage.

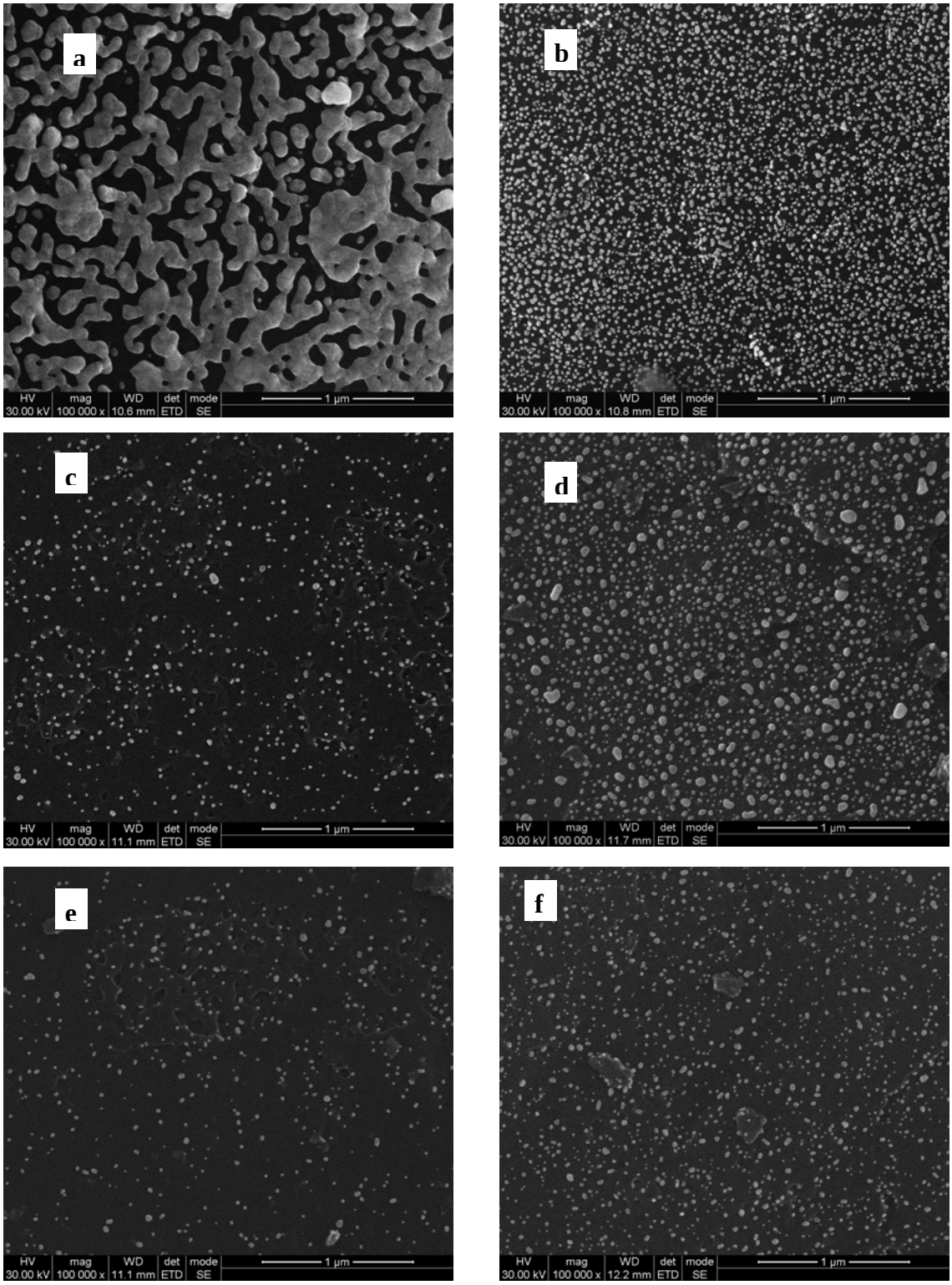

Figure 2. Fe-SEM micrographs of the sorbents, Au particle size distribution and circularity of the Au particles : a) MC-orig-Au-HC; b) MC-orig-Au-SMC; c) MC-orig-Au-C2; d) MC-HNO3-Au-C2; e) MC-air-Au-C2; f) MC-vapor-Au-C2.

3.3. Mercury retention-regeneration tests

Blank experiments on the supports were carried out in order to test the influence of them on the retention capacity of the Au-based sorbents. These experiments were performed according to the conditions described in the experimental section.

Figure 3a depicts breakthrough curves for supports and the amount of Hg captured (from integration of the breakthrough curves, deducting death volume of the reactor) is given in Table 3. As can be seen all the supports have some ability for Hg retention, in particular, the support treated with nitric acid, MC-HNO3. However, these supports cannot be considered for blank experiments. The reason is that once Au is deposited, a reducing treatment is applied to the sorbents, so the real blank is a support that undergoes the same reducing treatment. Thus, reduced supports (labelled as –red) were tested for Hg retention capacity.

Figure 3b depicts Hg breakthrough curves for reduced supports and the amount of Hg captured is given in Table 3. As can be seen, the breakthrough time is in the range of few minutes and the amount of Hg captured is negligible, except for support MC-HNO3-red. The reason for the behaviour of the support treated with nitric acid (as prepared and reduced) can be explained in terms of surface chemistry of this support. As can be deduced from Table 1, this support has incorporated a high amount of CO_2-evolving groups, which could chemisorb Hg. Once the support has been reduced, part of these groups disappears and less active sites for Hg chemisorption are available. However, after reduction, this support has still some Hg retention capacity (higher than the other reduced supports). This fact can be explained in terms of the temperature during reduction treatment. The reduction of support MC-HNO3 was carried out at 300ºC and the necessary temperature to remove most of the CO_2-evolving groups is around 400ºC. In order to check this hypothesis, MC-HNO3 exhausted support was undergone to a TPD to follow the evolution on the Hg adsorbed onto the support After complete desorption an experiment of Hg retention was carried out on the support. Figure 4 shows the Hg-TPD curve in which two peaks can be observed. First peak appears at 220ºC of temperature and can be attributed to Hg retained though physisorption mechanism. Second peak appears at 430ºC of temperature and can be attributed to Hg retained through chemisorption mechanism onto CO_2-evolving groups, which are removed completely near 550ºC. After Hg TPD experiment, a breakthrough curve for Hg was obtained for the regenerated support (MC-HNO3-reg), resulting in a negligible retention of Hg, as can be deduced from Table 3, obtaining similar values of Hg retention capacity than those obtained for the rest of the supports once reduced.

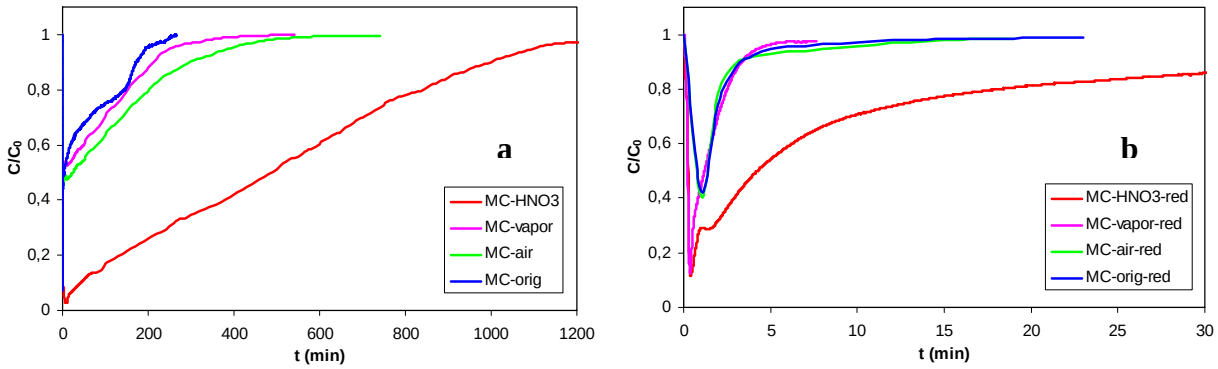

Figure 3. Mercury breakthrough curves for the supports (as prepared and reduced in H_2/Ar)

Table 3 . Total amount of Hg captured by the supports

Support	Hg captured [a] (µg/g support)	Hg captured [b] (µg/g support)
MC-orig	9.94	
MC-HNO3	87.86	81.69
MC-vapor	26.40	
MC-air	12.19	
MC-orig-red	0.26	
MC-HNO3-red	2.62	
MC-vapor-red	0.58	
MC-air-red	0.24	
MC-HNO3-reg	0.39	

[a] from integration of breakthrough curves
[b] direct determination on the exhausted support by mercury analyzer

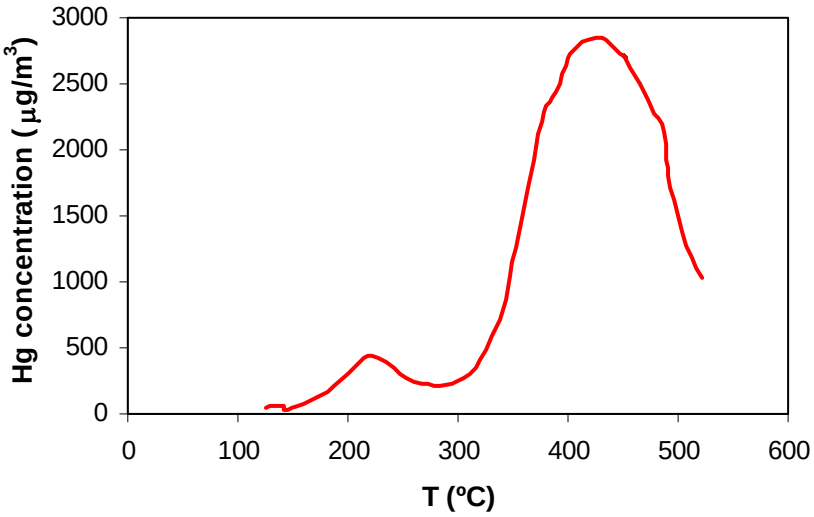

Figure 4 . Hg temperature programmed desorption for exhausted support MC-HNO3.

Figure 5 depicts the breakthrough curves for the Au/C sorbents and Table 4 summarizes the total amount of Hg retained on the sorbents (calculated from the integration of the breakthrough curves). First noticeable observation is the reproducibility of the experiments, taken into account that the inlet Hg concentration is as low as 22 ppbv (200 µg/m^3).

As can be deduced from Table 4 there is not a direct relationship between Au content and Hg capture capacity of the sorbents. This fact means that not all the Au deposited on the supports is efficient for Hg capture. The size of the Au nanoparticles has a big influence on the Hg capture efficiency, as can be seen in Figure 6. Despite it is not possible to calculate Au particle size of sorbent MC-orig-Au-SHC, its efficiency for mercury retention has been added into this Figure, out of scale, only for comparison purpose. It seems clear that there is a compromise between the amount of Au on the surface and the particle size reached. So, efforts have to be focused on the development of a sorbent with high Au content on the surface and an appropriate Au particle size.

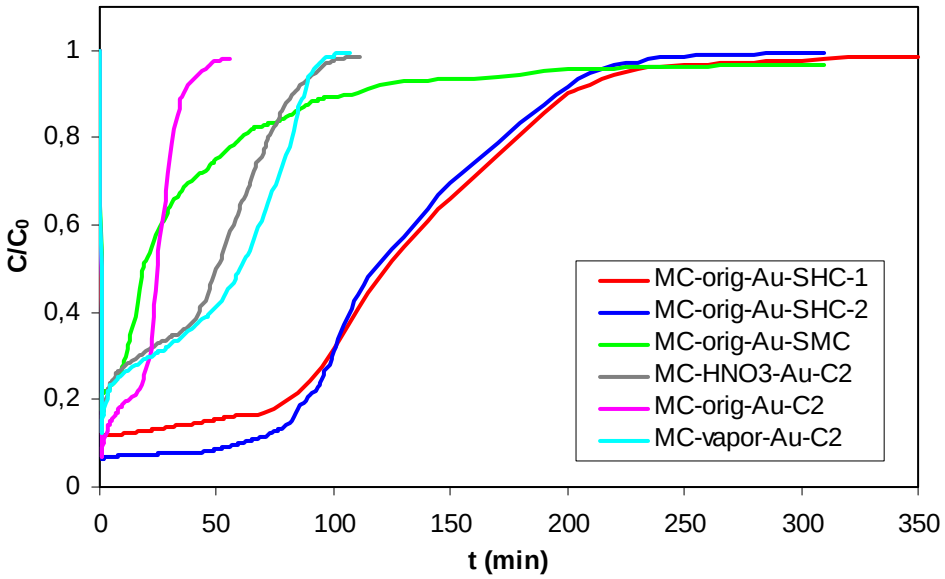

Figure 5. Mercury breakthrough curves for the sorbent.

Table 4 . Total amount of Hg captured by the sorbents

Sorbent	Hg captured (μg/g sorbent)
MC-orig-Au-SHC-1	29.7
MC-orig-Au-SHC-2	29.0
MC-orig-Au-SMC	10.8
MC-orig-Au-C2	5.7
MC-HNO3-Au-C2	10.1
MC-air-Au-C2	6.0
MC-vapor-Au-C2	12.1

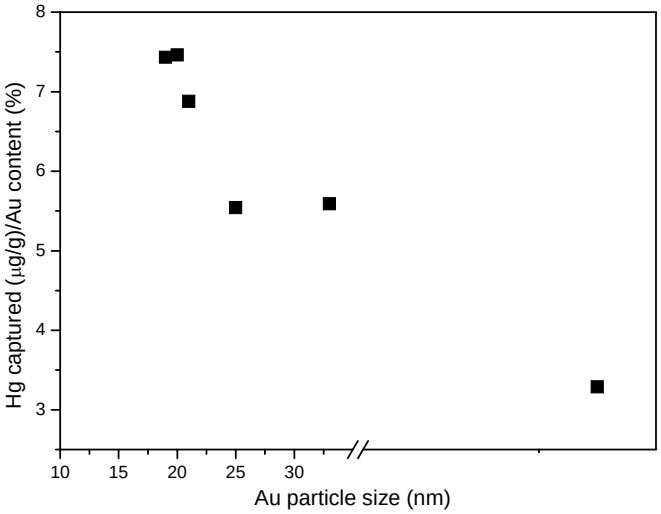

Figure 6. Relationship between Hg captured by the sorbents and the amount of Au and its particle size

Exhausted sorbents were undergone to a TPD to follow the evolution of the Hg adsorbed onto the sorbents in order to test the optimum temperature for regeneration. Figure 7 shows Hg-TPD curves for some sorbents. The mechanism for Hg retention onto the sorbents is different from that showed for support MC-HNO3 as can be deduced from Figures 7 and 4. The mechanism of chemisorption is very limited after removing CO_2-evolving groups (sorbents have all been reduced at 300ºC in H_2 atmosphere) from supports, as can be deduced from the total amount of Hg captured given in Table 3. So, the mechanism for Hg retention could be attributable to the amalgamation with Au nanoparticles. This fact is very significant, because temperatures for regeneration of sorbents are lower than for support MC-HNO3 and do not depend on the surface chemistry of the sorbents. The inspection of the Hg-TPD curves can help to fix regeneration conditions for the sorbents as 220ºC and held time of 2 h.

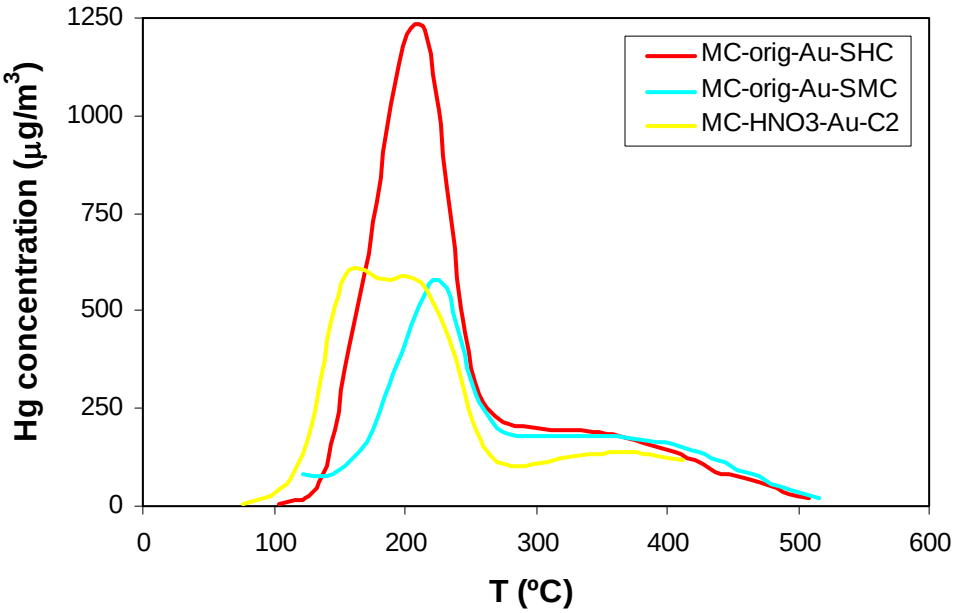

Figure 7. Hg temperature programmed desorption for exhausted sorbents

4. Conclusions

Regenerable sorbents based on Au deposition on structured carbon-based monoliths has been tested to determine the Hg capture capacity as well as their regenerability. Main conclusions deal with the importance of the relation of Au content and Au particle size and the mechanism of regeneration of the sorbents.

From this preliminary study, a compromise between the amount of Au on the surface and the particle size reached during gold deposition can be found. On the other hand, the regeneration of the Hg exhausted sorbent can be carried out at low temperature if the absence of CO_2-evolving groups (from TPD) is guaranteed. Further research concerning the preparation of sorbents with lower Au particle size is needed.

Acknowledgements

The financial support from Spanish Ministry of Science and Innovation (ref: CTQ2008-06860-C02-02/PPQ) is duly recognized.

References

[1] UNEP Chemical Branch, 2008. The Global Atmospheric Mercury Assesment: Sources, Emissions and Transport. UNEP-Chemicals, Geneva.
[2] http://www.epa.gov/mercury/regs.htm
[3] European Commision. Brussels 28.01.05 COM (2005) 20 final SEC(2005) 101.
[4] European Union emission inventory report 1990-2008 under the UNECE Convention on Long-range Transboundary Air Pollution (LRTAP). EEA Technical Report 7/2010. Copenhagen, 2010.
[5] Olson, E. S.; Mibeck, B. A. Oxidation Kinetics and the Model for Mercury Capture on Carbon in Flue Gas, International Conference on Air Quality V, Arlington, VA, September 19-21, 2005
[6] Long, S. J.; Scott, D. R.; Thompson, R. J. Atomic absorption determination of elemental mercury collected from ambient air on silver wool. Anal. Chem. 1973, 45, 2227–2233.
[7] Nowakowski, R.; Kobiela, T.; Wolfram, Z.; Duoes, R. Atomic force microscopy of Au/Hg alloy formation on thin Au films. Appl. Surf. Sci. 1997, 115, 217–231.
[8] Schaedlich, F. H.; Schneeberger, D. R. Cartridge for Collection of a Sample by Adsorption onto a Solid Surface. U.S. Patent 5660795, 1997.
[9] Levlin, M.; Ikävalko, E.; Laitinen, T. Adsorption of mercury on gold and silver surfaces. J. Anal. Chem. 1999, 365, 577–586.
[10] Battistoni, C.; Bemporad, E.; Galdikas, A.; Kacˇiulis, S.; Mattogno, G.; Mickevicˇius, S.; Olevano, V. Interaction of mercury vapour with thin films of gold. Appl. Surf. Sci. 1996, 103, 107–111.
[11] Yan, T. Y. A novel process for Hg removal from gases. Ind. Eng. Chem. Res. 1994, 33, 3010–3014.
[12] R. Juan, M.T. Izquierdo, C. Ruiz, B. Rubio. Preparation and Characterization of Carbon-Based Regenerable Sorbents for Mercury Retention. Carbon'2009. Internacional Conference on Carbon. Biarritz, France.
[13] Turkevich, J; Stevenson, PC; Hillier, J. A study of the nucleation and growth processes in the synthesis of colloidal gold. Discuss. Faraday Soc. 1951, 11, 55-75.
[14] Noh J.S., Schwarz J.A. Effect of HNO_3 treatment on the surface-acidity of activated carbons. Carbon 1990, 28, 675-682.
[15] Bansal R.C., Donnet J.B., Stoeckli. F., 1988. Active Carbon. Marcel Dekker. NY.
[16] Jiang L., Gao, L. Modified carbon nanotubes: an effective way to selective attachment of gold nanoparticles. Carbon 2003, 41, 2923–2929.